DIAMOND, R. (1971). *Acta Cryst.* **A27**, 436-452.
DODSON, E. J. (1985). In *Molecular Replacement*, edited by P. A. MACHIN, pp. 33-45. Warrington: SERC Daresbury Laboratory.
ELY, K. R., GIRLING, R. L., SCHIFFER, M., CUNNINGHAM, D. E. & EDMUNDSON, A. B. (1973). *Biochemistry*, **12**, 4233.
FITZGERALD, P. M. D. (1988). *J. Appl. Cryst.* **21**, 273-278.
GAYKEMA, W. P. J., HOL, W. G. J., VEREIJKEN, J. M., SOETER, N. M., BAK, H. J. & BEINTEMA, J. J. (1984). *Nature (London)*, **309**, 23-29.
HOGLE, J. M., MAEDA, A. & HARRISON, S. C. (1986). *J. Mol. Biol.* **191**, 625-638.
HOLDEN, H. M., RYPNIEWSKI, W. R., LAW, J. H. & RAYMENT, I. (1987). *EMBO J.* **6**, 1565-1570.
JONES, A. (1985). *Methods Enzymol.* **115**, 157-171.
JONES, E. Y., STUART, D. I. & WALKER, N. P. C. (1989). *Nature (London)*, **338**, 225-228.
KABSCH, W. (1976). *Acta Cryst.* **A32**, 922-923.
LADENSTEIN, R., BACHER, A. & HUBER, R. (1987). *J. Mol. Biol.* **195**, 751-753.
LESLIE, A. G. W. (1989). In *Improving Protein Phases*, edited by S. BAILEY, E. DODSON & S. PHILLIPS, pp. 13-24. Warrington: SERC Daresbury Laboratory.
LUO, M., VRIEND, G., KAMER, G., MINOR, I., ARNOLD, E., ROSSMANN, M. G., BOEGE, U., SCRABA, D. G., DUKE, G. M. & PALMENBERG, A. C. (1987). *Science*, **235**, 182-191.
MUIRHEAD, H., COX, J. M., MAZZARELLA, L. & PERUTZ, M. F. (1967). *J. Mol. Biol.* **28**, 117-150.
O'HALLERAN, T., LIPPARD, S. J., RICHMOND, T. J. & KLUG, A. (1987). *J. Mol. Biol.* **194**, 705-712.
OLD, L. J. (1987). *Nature (London)*, **326**, 330-331.
PETSKO, G. A. (1985). *Methods Enzymol.* **114**, 147-156.
RAYMENT, I. (1983). *Acta Cryst.* **A39**, 102-116.
ROSSMANN, M. G., ARNOLD, E., ERICKSON, J. W., FRANKENBERGER, E. A., GRIFFITH, J. P., HECHT, H.-J., JOHNSON, J. E., KAMER, G., LUO, M., MOSSER, A. G., RUECKERT, R. R., SHERRY, B. & VRIEND, G. (1985). *Nature (London)*, **317**, 145-153.
ROSSMANN, M. G. & BLOW, D. (1962). *Acta Cryst.* **15**, 24-31.
STUART, D. I., LEVINE, M., MUIRHEAD, H. & STAMMERS, D. K. (1979). *J. Mol. Biol.* **134**, 109-142.
TANAKA, N. (1977). *Acta Cryst.* **A33**, 191-193.
WALKER, N., MARCINOWSKI, S., HILLEN, H., MACHTLE, W., JONES, E. Y. & STUART, D. (1990). *J. Cryst. Growth*, **100**, 168-170.
WANG, B. C. (1985). *Methods Enzymol.* **115**, 90-111.

Acta Cryst. (1991). **A47**, 770-775

Extinction Effects in Polarized Neutron Diffraction from Magnetic Crystals. I. Highly Perfect MnP and YIG Samples

BY JIŘÍ KULDA*

Nuclear Physics Institute, ČSAV, 250 68 Řež near Prague, Czechoslovakia

JOSÉ BARUCHEL

Institut Laue-Langevin, 156X, 38042 Grenoble CEDEX, France, and Laboratoire Louis Néel, CNRS/UJF, 166X, 38042 Grenoble CEDEX, France

AND JEAN-PIERRE GUIGAY AND MICHEL SCHLENKER

Laboratoire Louis Néel, CNRS/UJF, 166X, 38042 Grenoble CEDEX, France

(*Received* 12 *November* 1990; *accepted* 11 *June* 1991)

Abstract

Wavelength-dependent flipping-ratio data obtained with polarized neutrons are analysed with the help of two extinction models: Kato's [*Acta Cryst.* (1980), **A36**, 763-769, 770-776] statistical dynamical theory (SDT) and the random elastic deformation (RED) approach [Kulda (1987). *Acta Cryst.* **A43**, 167-173; (1991). *Acta Cryst.* **A47**, 775-779]. Because the crystals used were nearly perfect, *Pendellösung* oscillations are present in all cases and the extinction theories are thus tested under extreme conditions. Both treatments give fair agreement with the experimental data in the short-wavelength range and there is no significant difference between them in terms of the goodness of fit, but the parameters involved in the RED approach have a more straightforward physical meaning. There are, however, inconsistencies in the values of the SDT parameters obtained, as well as probable deviations at large wavelength and crystal thickness, which could be related to a new validity condition for SDT.

1. Introduction

The problem of adequate correction of observed Bragg reflection intensities for the effect of extinction, *i.e.* reduction with respect to the prediction of the kinematical theory, has been subject to continuous efforts of both theorists and experimentalists for many years. In the last decade the availability of a statistical diffraction theory (SDT) capable, in principle, of dealing with the whole range of crystal perfection (Kato, 1976, 1980) has spurred a few experimental

* Present and permanent address: Institut Laue-Langevin, 156X, 38042 Grenoble CEDEX, France.

0108-7673/91/060770-06$03.00

measurements using X-rays (Olekhnovich, Karpei, Olekhnovich & Puzenkova, 1983; Voronkov, Piskunov, Chukhovskii & Maximov, 1987) and γ-rays (Schneider, Goncalves & Graf, 1988; Schneider, Goncalves, Rollason, Bonse, Lauer & Zulehnder, 1988), and another theoretical approach, the random elastic deformation (RED) model, has been proposed by one of the present authors (Kulda, 1987, 1989, 1991). This paper reports a test of both theories using polarized neutrons and magnetic crystals.

This kind of experiment is well suited to the investigation of extinction effects as the data consist, for each reflection, of intensities corresponding to two different structure-factor values $F_G^+ = F_{GN} + F_{GM}$ and $F_G^- = F_{GN} - F_{GM}$ (sum and difference of the nuclear and magnetic structure factors, respectively). Although the primary data which should ideally be compared to theory are the absolute integrated reflectivities, we do not feel confident enough of their values. We therefore prefer to restrict ourselves to the results on the variation with wavelength of the flipping ratio R_f, the ratio of the integrated reflectivities corresponding to the two polarization states of the incident neutron beam.

2. The data

We have chosen the results of measurements of the wavelength dependence of the flipping ratio R_f on several high-quality ferro- and ferrimagnetic crystals, performed at the ILL, Grenoble. The particular data sets are labelled as follows:

YIG1 - data from a 0·495 (2) mm thick (112) yttrium iron garnet crystal reported previously by Baruchel, Guigay, Mazuré-Espejo, Schlenker & Schweitzer (1982). A highly perfect part of the crystal was chosen on the basis of X-ray topographic work to enable observation of the magnetic *Pendellösung* oscillations on the $2\bar{2}0$ reflection.

YIG0 - data collected by the above authors from a thin slice of the same material in which growth striations were again parallel to the surface but with the whole volume of the sample irradiated. The thickness was 0·1 mm and the reflection was again $2\bar{2}0$.

MNP - data obtained by Guigay, Baruchel, Schlenker, Schweitzer & Patterson (1986) with a (100) MnP crystal plate in the ferromagnetic phase (temperature 60 K), the thickness varied between 70 and 85 μm and the 020 reflection was used.

All the measurements were performed in symmetrical transmission geometry with incident-beam polarization parallel to the magnetization and perpendicular to the scattering vector. At each wavelength integrated intensities were measured for both spin orientations and corrected for background. The magnitude of the $\lambda/2$ contamination was checked experimentally and proved negligible in all cases. The absolute uncertainties on R_f estimated from the counting statistics alone vary between 0·005 and 0·02 for $\lambda < 1{\cdot}05$ Å and amount to 0·05 elsewhere. For YIG0 the observation of the scatter indicates, however, that the uncertainty is somewhat underestimated.

3. The extinction models

All three data sets chosen for the present study exhibit local maxima and minima in the observed $R_f(\lambda)$ dependences. The most natural interpretation in view of the high quality of the samples known from X-ray topographic work is that the diffraction process is strongly influenced by a dynamical effect, *Pendellösung* interference. This limits the choice of possible extinction models for the data treatment to only two variants: the statistical dynamical theory (SDT) developed originally by Kato (1976, 1980) and the random elastic deformation model (RED) suggested by one of the present authors (Kulda, 1987, 1989, 1991). Traditional approaches based on the energy transfer equations (ETE) refer from the very beginning to intensities only and hence they are not capable of properly covering effects arising from interference of the waves propagating inside a crystal. In this section we give a brief account of the basic assumptions of both models and of the most important formulas for their implementation. Symmetric transmission geometry and plane-parallel samples of thickness t with the effective beam path given by $T = t/\cos\Theta$ are assumed.

Kato's model (*SDT*)

This was implemented including the latest improvements due to Al Haddad & Becker (1988) and Guigay (1989). According to this approach the intensity diffracted by a crystal of arbitrary quality consists of three components. In the case of an infinite plate and symmetric transmission geometry the coherent part of the integrated reflectivity, expressed in terms of the reduced deviation from the Bragg angle y, is given by

$$\rho_y^c = (\pi/2)EW(2EA)\exp[-(1-E^2)\alpha_c A] \quad (1)$$

where A is the effective beam path T scaled by the extinction length $\Delta_G = \Omega/F_G\lambda$ (Ω being the unit-cell volume) and W represents the Waller function, $W(x) = \int_0^x J_0(\xi)\,d\xi$. For $E = 1$, (1) yields the result of dynamical theory for a perfect crystal. The 'static' Debye–Waller factor E characterizes lattice disorder due to local strain fields while $\alpha_c = 2\tau_c/\Delta_G$ is the coherent phase correlation length scaled to the extinction length. The purely incoherent contribution is a solution to a set of intensity-coupling equations, similar to those used within the mosaic model, describing mutually independent multiple rescattering events characterized by the effective correlation length τ_e. We shall put $\alpha_e = 2\tau_e/\Delta_G$ and write

$$\rho_y^i = (\pi/2)(1-E^2)[1-\exp(-2\alpha_e A)]/\alpha_e. \quad (2)$$

Finally, the mixed part representing waves subject to a transition from the coherent channel into the incoherent one can be expressed as

$$\rho_y^m = (\pi/2)E(1-E^2)\alpha_c \exp(-2\alpha_e A)$$
$$\times \int_0^A \exp\{-[(1-E^2)\alpha_c - 2\alpha_e]a\}$$
$$\times (Ea\{\exp[2\alpha_e(A-a)]+1\} - W(2Ea))\,da. \tag{3}$$

The integrated reflectivity is then $\rho_y = \rho_y^c + \rho_y^i + \rho_y^m$.

RED - primary extinction

Unlike the original variant of the RED formalism (Kulda, 1987) the beam path in the crystal is assumed always to fall into a single deformed domain so that no secondary extinction originating from subsequent interaction with different domains may arise. As discussed elsewhere (Kulda, 1989, 1991), the final solution in this case is formed by averaging the reflectivities, supplied by the dynamical theory, over an ensemble of domains characterized by probability distributions of the local values of the crystal thickness and of the bending radius.

As outlined in the companion paper (Kulda, 1991), a reasonable choice for the description of the thickness fluctuations may be the Gaussian distribution

$$w_1(t) = (\pi^{1/2}\Delta t)^{-1} \exp[-(t-\bar{t})^2/\Delta t^2]. \tag{4}$$

For the bending radius spread the γ distribution seems more convenient. We write

$$w(\eta) = \eta^\alpha e^{-\eta}/\Gamma(\alpha+1) \tag{5}$$

with $\eta = (\alpha+1)R/\bar{R}$. For a given mean effective bending radius $\bar{R}$, both its shape and its variance $[\bar{R}^2/(\alpha+1)]$ depend on the parameter α. The γ distribution comprises a simple exponential and a near Gaussian as two limiting cases corresponding to $\alpha = 0$ and $\alpha \gg 1$, respectively.

The averaged integrated reflecting power is then given, using the results of Chukhovskii & Petrashen' (1977), by

$$\bar{\rho}_y = \pi \int_0^\infty dR \int_0^\infty dA \int_0^A da$$
$$\times |{}_1F_1(-i/2\nu, 1, -2i\nu a(a-A))|^2 w_1(t) w_2(R). \tag{6}$$

Here again $A = t/\Delta_G \cos\Theta$ and $\nu = \partial Y/\partial A$ is the local reduced deformation gradient related to the effective bending radius R by

$$\nu = C(c, \Theta)/Q_{\rm kin}R \tag{7}$$

where $Q_{\rm kin} = |F_G|^2\lambda^3/\Omega^2 \sin 2\Theta$ is the kinematical reflecting power and the function

$$C(c, \Theta) = c \tan\Theta \sin\Theta + (1-c)\cos\Theta$$

approximates the possible angular variation of the deformation gradient for various deformation types (Kulda, 1991). The integrations of (6) have to be performed numerically.

4. Data evaluation and results

For confrontation with experimental results, the $\bar{\rho}_y$ have to be converted to the angular scale by multiplication by a factor which for the rotating-crystal method can be written as $H_G = |F_G|\lambda^2/\pi\Omega \sin 2\Theta$. In the expression for the flipping ratio most of the parameters cancel out so that we arrive at

$$R_f = (|F_G^+|/|F_G^-|)\bar{\rho}_y^+/\bar{\rho}_y^-. \tag{8}$$

It is the second term which in the presence of *Pendellösung* oscillations may fall on either side of unity, giving rise to a non-monotonic variation of $R_f(\lambda)$. Such behaviour is illustrated in Fig. 1 which displays the reduced beam path A, the mean reduced deformation gradient $\bar{\nu}$ (corresponding to $\bar{R}$) and the integrated reflecting power $\bar{\rho}_y$ evaluated with the best-fit parameters for the YIG0 data and the RED model.

A purpose-written computer code *FLIRT* based on a Marquardt-Levenberg non-linear least-squares minimization algorithm (*cf. e.g.* Press, Flannery, Teukolsky & Vetterling, 1986) was employed to fit the observed flipping-ratio data by the model given by (8). Two groups of free parameters were refined simultaneously: those of a particular extinction model and those related directly to the sample. For RED we refined the effective mean bending radius $\bar{R}$, the parameter c governing the angular variation of the deformation gradient and the parameter α of the γ distribution. With Kato's SDT we have used as free parameters the static Debye-Waller factor E and the two correlation lengths, τ_c and τ_e, taken as independent. In addition there were the model-independent parameters: the magnetic structure factor F_M and for

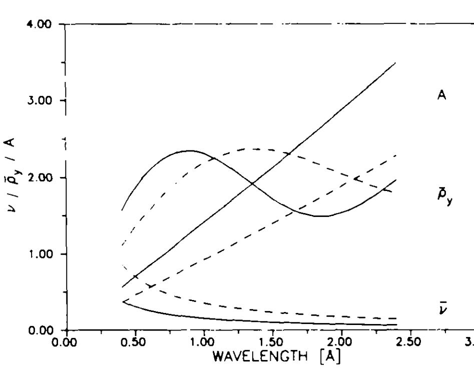

Fig. 1. The reduced beam path A, the averaged reduced deformation gradient $\bar{\nu}$ and the integrated reflectivity $\bar{\rho}_y$ calculated for parameter values refined for the YIG0 data and the RED model. The full and dashed lines correspond to F_{220}^+ and F_{220}^-, respectively.

the MNP data also the effective crystal thickness and its relative spread $\Delta t/t$ which were difficult to be determined independently because of the irregular shape of the sample.

To speed up the computation, tables of integrated reflectivities for ranges of low A and $\bar{\nu}$ values, where dynamical effects play an important role (*cf.* Fig. 1),

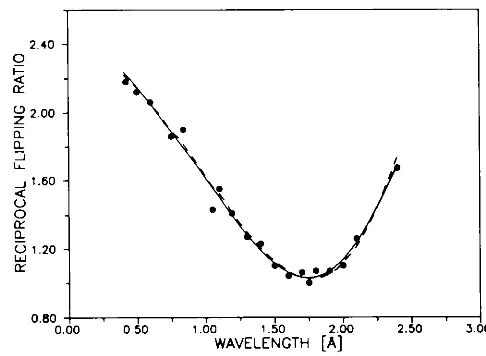

Fig. 2. Observed values of the flipping ratio (●) and the theoretical curves fitted according to the RED (full line) and SDT (dashed line) models for the YIG0 sample.

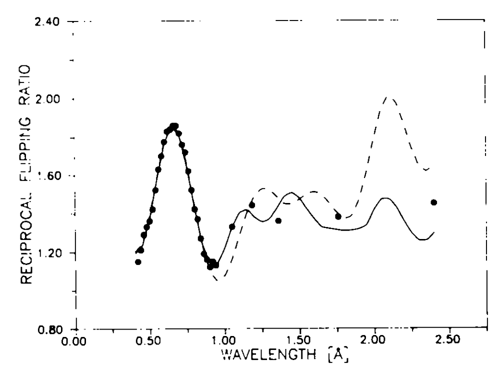

Fig. 3. Observed values of the flipping ratio (●) and the theoretical curves fitted according to the RED (full line) and SDT (dashed line) models for the YIG1 sample.

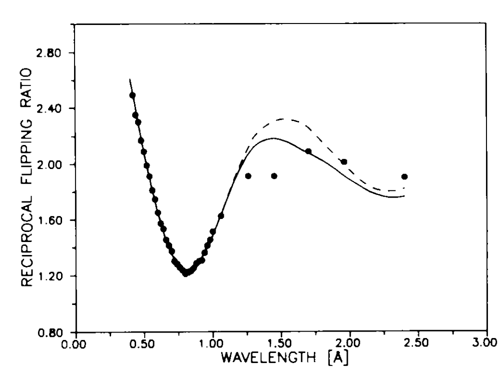

Fig. 4. Observed values of the flipping ratio (●) and the theoretical curves fitted according to the RED (full line) and SDT (dashed line) models for the MNP sample.

Table 1. *Fitted parameters and χ^2 values for the RED model; asterisks indicate the values kept fixed during the fit*

Data	YIG0	YIG1	MNP
F_N (10^{-12} cm)	4·56*	4·56*	2·94*
F_M (10^{-12} cm)	21·7 (2)	19·7 (1)	0·987 (7)
$\bar{t}$ (μm)	100*	495*	82·4 (3)
$\Delta t/\bar{t}$	0*	0·005*	0·21 (1)
α	0·8 (6)	1·4 (2)	2·4 (7)
$\bar{R}(m)$	2·5 (9)	14·1 (4)	15 (2)
c	1·0 (1)	0·983 (1)	0·77 (3)
χ^2	5·22	1·34	0·89

Table 2. *Fitted parameters and χ^2 values for the SDT model; asterisks indicate the values kept fixed during the fit*

Data	YIG0	YIG1	MNP
F_N (10^{-12} cm)	4·56*	4·56*	2·94*
F_M (10^{-12} cm)	21·9 (2)	23·1 (1)	0·982 (6)
$\bar{t}$ (μm)	100*	495*	83·7 (3)
$\Delta t/\bar{t}$	0*	0·005*	0·23 (1)
E	0·96 (2)	0·88 (1)	0·972 (2)
τ_c (μm)	13 (3)	0·37 (5)	0·1 (2)
τ_{c_2} (μm)	20 (13)	17 (1)	48 (4)
χ^2	4·99	4·97	1·10

were generated in advance and interpolation was used in the course of the fit to retrieve the required ρ values for RED and the Waller functions for SDT. In this way the time required for a single cycle of refinement on six parameters with 30 data points was cut down to a few minutes on a PC/AT 286/287 system running at 12 MHz; usually about five cycles were required for convergence to the minimum of χ^2.

When displaying the final results in Figs. 2–4 we plot $1/R_f$ instead of R_f to make visualization easier while remaining consistent with the relative phases of the nuclear and magnetic structure factors. The fitted parameters are given in Tables 1 and 2. Only with YIG1 is there a significant difference in terms of the goodness of fit between the results obtained by means of RED and SDT.

The figures show that the agreement between observed and calculated values is good in the low-wavelength part of the results and doubtful at higher wavelengths. Two reasons may be found for this. Firstly, the role of extinction increases with wavelength and so does the sensitivity to any inadequacies of the models. Secondly, the low-wavelength part is much more heavily weighted during the fitting procedure due to the much larger number of experimental points and lower estimated errors. Hence the fit automatically favours this part. This inconsistency in our experimental strategy occurs because polarized-neutron instruments with continuously tunable wavelength and an excellent technology for flipping-ratio measurements are available only for the hot neutron range: the instrument used for the measurements described was D5. The points at wavelengths above 1·05 Å were measured on S20, a simple instrument less suited for quantitative polarized neutron work, located on a thermal neutron guide tube, hence with a serious problem of $\lambda/2$ contributions between 1·8 and 2·4 Å (at 2·4 Å a graphite filter is operative). The rather scarce experimental points in the higher-wavelength region are satisfactorily accounted for in the case of the thin YIG crystal (Fig. 2), but Figs. 3 and 4 indicate that the description in the other cases is not very good.

5. Discussion

Although for the MNP and YIG0 as well as the low-wavelength part of the YIG1 data sets the RED formalism does slightly better than SDT, the differences in χ^2 are never significant, even if attributed to a single free parameter. This is somewhat surprising in view of the quite profound differences in the basic assumptions of the two models. One has, however, to bear in mind that all of the data correspond to a short range of low values of the reduced beam path where the integrated intensity curves calculated according to SDT and RED may well approximate each other. In the long-wavelength part of the YIG1 data the differences between the two appoaches gain in importance, but the presently available data are too sparse for definite conclusions to be drawn.

The consistency of the refined free parameter values with the model assumptions and with physical reality can be checked quite easily with RED which has from its very beginning been built in analogy with the well understood process of diffraction in elastically deformed crystals. Indeed, all the final values of the $\bar{R}$, c and α parameters given in Table 1 appear quite realistic. The corresponding 'mosaic spread' $\delta\Theta \simeq T/\bar{R}$ is then of the order of a few seconds of arc for all of the samples, allowing for the presence of dynamical diffraction effects. The fact that the c values do not deviate much from unity implies a tendency to a $\tan\Theta/\bar{R}$ behaviour for the deformation gradient characteristic for lattice-parameter variation. The α values do not strongly exceed unity, confirming the need for an asymmetric distribution of the bending radii, which allows for the fact that, within certain limits, the larger the deformation gradient (smaller bending radius) in a domain, the smaller may be its size to produce a given contribution to the sample's total reflectivity. As a consequence the more deformed domains may be present in larger numbers and the corresponding bending radii have to be more heavily weighted in the distribution function.

The physical meaning of the parameters of SDT (Table 2) is, at least for long-range distortions, more difficult to visualize. To facilitate a detailed discussion one would have to create first a plausible model and calculate for it the phase correlation function to establish the links of E, τ_c and τ_e to the crystal properties. To our knowledge this has not yet been done. In general, the static Debye–Waller factor E should approach unity for highly perfect crystals so that the coherent component of the diffracted intensity could play a substantial role. The present results confirm this. The refined values of the coherent correlation length τ_c are small enough to obey both the basic condition $\tau_c \ll \Delta_G$ as well as the new relation $\tau_c T \ll \Delta_G^2$ derived recently by Guigay (1991).

Important difficulties appear, however, when we analyse the mutual relation between the correlation lengths τ_c and τ_e, which were treated as independent during the fits. The relation originally proposed by Kato (1980) implies that τ_e retains a finite value $E\Delta_G$ when $\tau_c \to 0$. Al Haddad (1989) and Becker & Al Haddad (1991) have shown this to be wrong and proposed a new relation yielding $\tau_e \to 0$ when $\tau_c \to 0$. The results of our fits tend to be in some disagreement with such behaviour. According to Table 2 we found τ_c very small (<1 μm) and τ_e much larger (17 μm for YIG1, 48 μm for MnP). Such contradictions were not reported in any of the previous successful tests of SDT by Olekhnovich *et al.* (1983), Voronkov *et al.* (1987), Schneider, Goncalves & Graf (1988) and Schneider, Goncalves, Rollason, Bonse, Lauer & Zulehnder (1988), the latter two being extensively referred to by Al Haddad (1989) and Becker & Al Haddad (1991). The fact that their samples contained predominantly point-like defects and separate dislocations suggests that SDT may not provide an equally adequate description of the diffraction by crystals containing few but extended (on the scale of Δ_G) defects (*e.g.* growth striations).

The most usual purpose for extinction corrections is the derivation of accurate structure factors. The behaviour of the present data is dominated by *Pendellösung* oscillations whose phase for an ideally perfect crystal is given by $\pi F_G \lambda T/\Omega$ and may provide highly accurate experimental estimates of F_G as λ and T are usually known with sufficient accuracy. This, however, is not true for deformed crystals where also the deformation gradient in RED and the static Debye–Waller factor E in SDT enter the period of the fringes. Therefore, in the present case of slightly imperfect crystals the derived values of F_G become quite sensitive to the accuracy with which a model describes the actual imperfections in the crystal. While from the MNP and YIG0 data reasonable magnetic structure-factor values were refined (Tables 1 and 2), the results for YIG1 always significantly differed from the values given by Bonnet, Delapalme, Fuess & Becker (1979). This outcome reflects the fact that the $R_f(\lambda)$ for the thin samples was measured in the range of the first *Pendellösung* maximum (*cf.* Fig. 1) where the diffracted intensity, although affected by extinction, does not strongly depend on deformation (Kulda, 1991). As soon as the data involve higher-order maxima (YIG1 in the present case) the situation rapidly changes.

One of the authors (JK) gratefully acknowledges the hospitality of the Institut Laue-Langevin, Grenoble, where a substantial part of this work has been done.

References

AL HADDAD, M. (1989). Thèse, Univ. Joseph Fourier, Grenoble, France.
AL HADDAD, M. & BECKER, P. (1988). *Acta Cryst.* **A44**, 262-270.
BARUCHEL, J., GUIGAY, J.-P., MAZURÉ-ESPEJO, C., SCHLENKER, M. & SCHWEITZER, J. (1982). *J. Phys. Colloq.* **43**, Suppl. 12, C7, 101-106.
BECKER, P. & AL HADDAD, M. (1991). *Acta Cryst.* In the press.
BONNET, M., DELAPALME, A., FUESS, H. & BECKER, P. (1979). *J. Phys. Chem. Solids*, **40**, 863-876.
CHUKHOVSKII, F. N. & PETRASHEN', P. V. (1977). *Acta Cryst.* **A33**, 311-?19.
GUIGAY, J.-P. (1989). *Acta Cryst.* **A45**, 241-244.
GUIGAY, J.-P. (1991). Unpublished.
GUIGAY, J.-P., BARUCHEL, J., SCHLENKER, M., SCHWEITZER, J. & PATTERSON, C. (1986). Report 5-16-107. Experimental Reports 1986, Institut Laue-Langevin, Grenoble, France.
KATO, N. (1976). *Acta Cryst.* **A32**, 458-466.
KATO, N. (1980). *Acta Cryst.* **A36**, 763-769, 770-776.
KULDA, J. (1987). *Acta Cryst.* **A43**, 167-173.
KULDA, J. (1989). *Physica (Utrecht)*, **B156 & 157**, 671-674.
KULDA, J. (1991). *Acta Cryst.* **A47**, 775-779.
OLEKHNOVICH, N. M., KARPEI, A. L., OLEKHNOVICH, A. I. & PUZENKOVA, L. D. (1983). *Acta Cryst.* **A39**, 116-122.
PRESS, W. H., FLANNERY, B. P., TEUKOLSKY, S. A. & VETTERLING, W. T. (1986). *Numerical Recipes*, ch. 14. Cambridge Univ. Press.
SCHNEIDER, J. R., GONCALVES, O. D. & GRAF, H. A. (1988). *Acta Cryst.* **A44**, 461-467.
SCHNEIDER, J. R., GONCALVES, O. D., ROLLASON, A. J., BONSE, U., LAUER, J. & ZULEHNDER, W. (1988). *Phys. Rev. B*, **29**, 661-674.
VORONKOV, S. N., PISKUNOV, D. I., CHUKHOVSKII, F. N. & MAXIMOV, S. K. (1987). *Sov. Phys. JETP*, **85**, 624-628.

Acta Cryst. (1991). **A47**, 775-779

The RED Extinction Model. III. The Case of Pure Primary Extinction

BY JIŘÍ KULDA*

Nuclear Physics Institute, ČSAV, 250 68 Řež near Prague, Czechoslovakia

(*Received* 12 *November* 1990; *accepted* 11 *June* 1991)

Abstract

Bragg diffraction in nearly perfect crystals is treated within the framework of the random elastic deformation (RED) model. Similar to the previous applications it is again assumed that each individual reflection event takes place within an elastically deformed domain and hence may be described by either an exact or a quasiclassical solution to the Takagi-Taupin equations. But because of the high degree of perfection and/or small thickness of the crystal the interaction is confined to one single domain so that the total reflected intensity is obtained just by summing up the contributions from the whole ensemble of domains characterized by different values of the deformation gradient and thickness. The present approach profoundly differs from Kato's statistical dynamical theory which starts with the averaging procedure within the Takagi-Taupin equations before solving them.

1. Introduction

The RED model was recently proposed (Kulda, 1987, 1988*a*) as an alternative to the mosaic model to describe extinction effects in imperfect crystals. Its main advantage was expected to arise from the more adequate treatment of the coherent part of the wave-crystal interaction. This expectation has been confirmed by the first practical tests (Kulda, 1988*b*) with neutron diffraction data collected on comparatively large (several mm) crystals of SrF_2, where both primary and secondary extinction seemed to play about equal roles.

At present we wish to examine to what extent this model, with appropriate specifications, is valid in situations of predominant primary extinction as is the case of thin crystal plates of comparatively high perfection, where the effective mosaicity may not exceed a few seconds of arc. This application range, besides practical aspects, appears important for two theoretical reasons. Firstly, it is interesting to find to what extent RED, with its emphasis on the deformed parts of the crystal, may adequately describe the behaviour of considerably perfect crystals. Secondly, it is just this kind of crystal to which Kato's theory of extinction (Kato, 1976, 1980; Guigay, 1989; Becker & Al Haddad, 1989, 1990) has been applied (*e.g.* Voronkov, Piskunov, Chukhovskii & Maximov, 1987; Al Haddad & Becker, 1988; Becker & Al Haddad, 1991) so that a direct comparison of the two approaches, each of them making a direct - yet different - use of the dynamical theory, becomes possible.

* Present and permanent address: Institut Laue-Langevin, 156X, 38042 Grenoble CEDEX, France.

0108-7673/91/060775-05$03.00